

Figure 1. Generalized surface geology map of Sabine Peninsula (after Harrison, 1994) displaying sedimentary stratigraphic divisions.

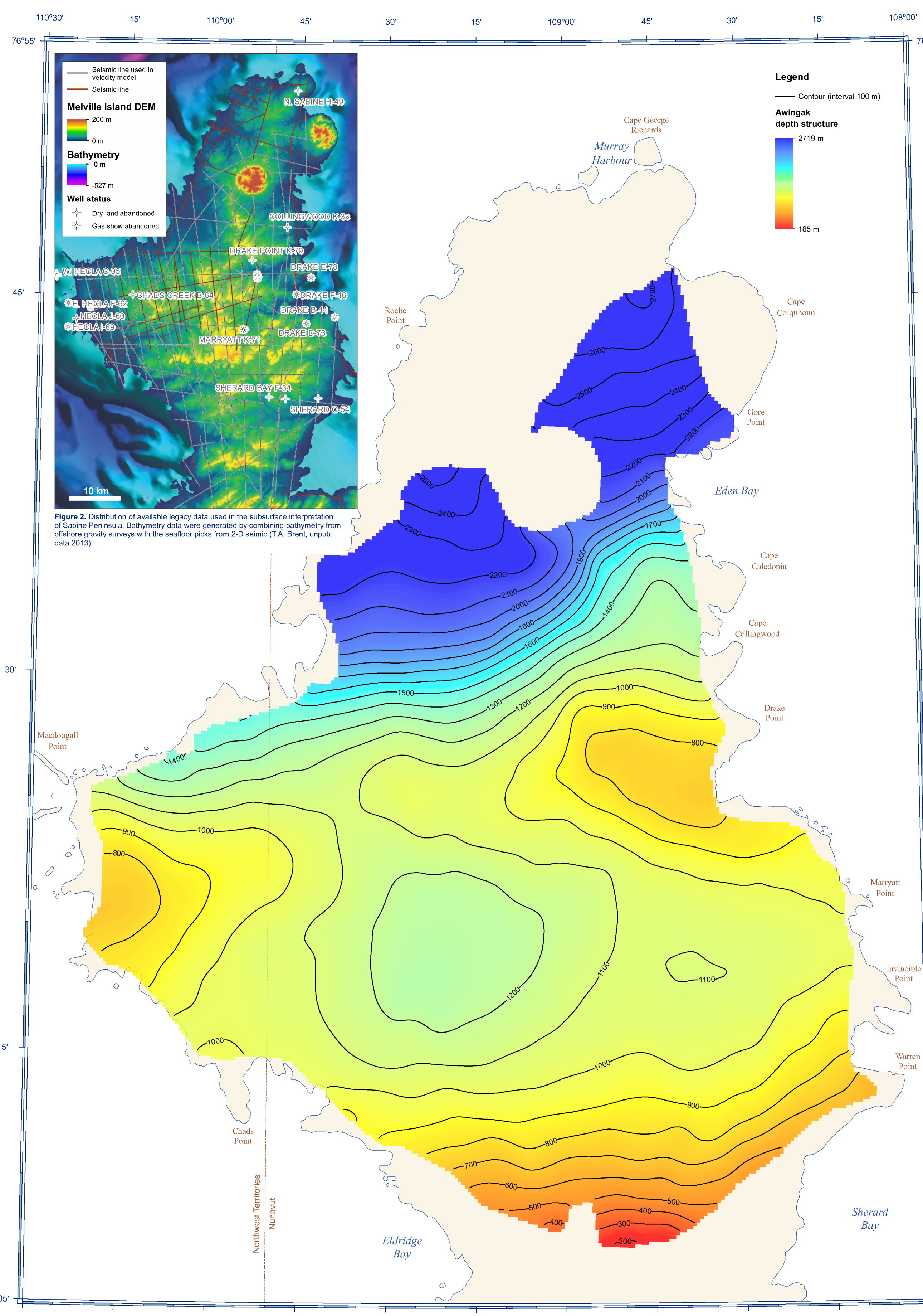


Figure 2. Distribution of available legacy data used in the subsurface interpretation of Sabine Peninsula. Bathymetry data were generated by combining bathymetry from offshore gravity surveys with the seafloor picks from 2-D seismic (T.A. Brent, unpub. data 2015).

INTRODUCTION

The time- and depth-structure maps presented herein are part of an eight-map series of the subsurface of Sabine Peninsula spanning the Early Permian through Early Cretaceous interval. These maps are the product of the application of modern geoscientific methods of processing and interpretation to a suite of legacy seismic-reflection data from onshore Sabine Peninsula (Melville Island, Western Arctic Islands). The resultant processed seismic lines were interpreted using the existing regional geological framework (see Harrison, 1995) by integrating existing regional well data, geophysical logs, age control, and the lithological information through synthetic seismograms.

REGIONAL SETTING

The Sabine Peninsula of Melville Island is located within the Sverdrup Basin in a northeast-southwest direction and is up to 350 km wide. The basin contains up to 13 km of sedimentary strata (Embry and Beauchamp, 2008). The Sverdrup Basin is separated from the underlying Franklinian Basin by an unconformity at the base of the Carboniferous strata. The Franklinian Basin was extensively redeformed following the Late Devonian–earliest Carboniferous Eiselemment Orogeny. The resulting rift-related structural depression acted as a major depocentre from the Carboniferous through the Paleogene (Embry and Beauchamp, 2008). The Sverdrup Basin succession was uplifted and deformed during the early Cenozoic Eurasian Orogeny. The surface geology of Melville Island is dominated by Lower Paleozoic strata of the Franklinian Basin. The Sabine Peninsula is an exception to this, as surface strata are part of the Sverdrup Basin. The geology of the Sabine Peninsula consists of deformed Late Carboniferous to Paleocene sandstone, siltstone, shale, and minor amounts of carbonate. Additionally, evaporitic rocks are exposed in two depocenters on northern Sabine Peninsula—the Barrow and Colquhoun domes, which consist of deformed anhydrite and gypsum. The strata of the Sverdrup Basin succession on Melville Island were deformed into a series of folds, including the Murray Harbour syncline to the north, the Drake Point anticline and the Maryatt Point syncline to the south (Harrison, 1994) (Fig. 1).

During a 1981 to 1983 phase of petroleum exploration, companies drilled 52 wells on Melville Island and surrounding waters (22 of which were on Sabine Peninsula) and acquired 3,400 line-kilometres of onshore seismic-reflection data (Fig. 2). Three separate gas fields were discovered in the Sabine Peninsula area: Drake Point, Hecla, and Roche Point. Feasibility studies for the development of the gas fields were conducted in the early 1980s; however, due to low gas prices and the lack of gas markets, the gas fields on Melville Island (and elsewhere in the Canadian Arctic) were not developed (Harrison, 1995).

SEISMIC DATA SET AND PROCESSING

Data access was obtained through a Memorandum of Understanding signed in 1997 by the Geological Survey of Canada (GSC), Panarctic Oils, the Arctic Islands Exploration Group, and the Offshore Arctic Exploration Group (joint-venture parties). The data sets consist of original land seismic-reflection field tapes transferred from 21-, 7-, and 5-track media. Data were collected using a dynamic charge of 20–30 kg per shot at about 20 m below the surface. Shot-point spacing ranged from 67 m to 200 m, the shorter spacing being used for most surveys. The majority of the seismic-reflection data were recorded using 48- or 96-channel systems. Channel stations were generally deployed using nine receivers spaced at about 5 m and station intervals varying from 50 m to 75 m. The common-midpoint multiplicity of the data sets range from single to 12-fold coverage. The most common recording length was 8 s.

The processing consisted of three main steps: 1) principal component decomposition was used to remove both coherent and random noise; 2) data were migrated utilizing poststack Kirchhoff migration; and 3) seismic bandwidths were extended to increase vertical resolution (Claproot et al., 2011; Duchesne et al., 2012).

Velocity model

A 3-D velocity model was built using about 1300 km of linear seismic data (78 lines) and 13 wells spread over an area of about 2800 km<sup>2</sup> (Fig. 2). The velocity model was then used for poststack migration processing and to convert seismic horizon surfaces from time to depth. The primary assumption behind the velocity model is that the coherent high-amplitude reflectors that were picked to build the model correspond to important acoustic-impedance contrasts caused by significant and abrupt velocity changes. This assumption was confirmed by tying seismic picks to well sonic logs (Duchesne et al., 2012). The geostatistical approach of kriging with an external drift (KED) was applied to both the reflection time of the picked seismic horizons, and time-depth surfaces derived from check shot data to compute the 3-D velocity field. Kriging interpolates values between the known positions based on weighted spatial correlations. The KED technique was specifically developed for the integration of seismic data into the kriging process where the number of wells is insufficient for the computation of adequate depth statistics (Hass and Dubrule, 1994). Hence, it uses the information provided by the time horizon picks to improve estimates where depth control is sparse. For seismic migration, root mean squared (RMS) velocity values are first estimated by KED from time-to-depth conversion of seismic horizon surfaces mapped as important velocity boundaries (Duchesne et al., 2012). Then, once the approximate depths of the surfaces are known, the interval velocities ( $V_{int}$ ) for all time intervals between two consecutive horizons are computed from:

$$V_{int} = \frac{\Delta z}{\Delta t}$$

where  $\Delta z$  and  $\Delta t$  are the depth and time intervals between two successive horizons  $i$ . Once  $V_{int}$  is obtained the RMS velocity ( $V_{rms}$ ) is calculated using:

$$V_{rms} = \sqrt{\frac{1}{N} \sum_{i=1}^N V_{int}^2 \Delta t_i}$$

in which  $N$  is the total number of horizons and  $\Delta t_i$  is the sum of all time intervals.

SEISMIC INTERPRETATION AND VISUALIZATION METHODS

Processed seismic lines were loaded into IHS-kingdom<sup>®</sup> seismic and geological interpretation software. Prominent seismic-reflection horizons, tied to well formation-top information, were manually correlated. Seed points were generated at seismic line intersections, thereby permitting the interpretation of adjacent lines.

The map would benefit from a detailed structural interpretation; however, confidence of this interpretation is minimized due to minor vertical offsets (about 0.1 s) attributed to faulting and the large line spacing. These reflections are vertically identified across fault-displacement offset.

Time-structure maps of the key seismic horizons were computed using universal kriging. Universal kriging permits the interpolation of a nonstationary, random field by adding a term in the kriging equation that accommodates any linear trends present in a scattered point set (Chilès and Dubrule, 1999). Given that our picked horizons showed a strong linear trend for time versus depth over distance, universal kriging provided the best fit to the picked horizons.

TIME TO DEPTH CONVERSION

All time surfaces are converted to depth using the following procedure. First  $V_{rms}$  of the 3-D velocity model are calculated using Dix equation:

$$V_{rms} = \left[ \frac{V_0^2 + \frac{1}{2} \sum_{i=1}^n (V_i^2 - V_{i-1}^2) \frac{t_i^2 - t_{i-1}^2}{t_i - t_{i-1}}}{t_n - t_0} \right]^{1/2}$$

where  $t$  is the zero-offset arrival time of the  $n$ th reflection. Interval limits corresponded to seismic horizons that are picked and tied to geological interfaces. Then  $V_{rms}$  are extracted from the velocity model along picked horizons. Velocity maps are then computed using Universal kriging at a cell size of 250 m. Finally, the time-structure surfaces of the various seismic horizons are converted to depth ( $Z$ ) using:

$$Z = \frac{t_n - t_0}{2}$$

Because the depth-conversion process is a function of the velocity model, the lateral extent of depth maps is confined to the lateral extent of the model. The final depth-structure maps were imported into ArcGIS for visualization using the Arc extension Team-GIS Bridge.

DESCRIPTIVE NOTES

Quantifying the uncertainty of seismic subsurface maps is difficult since several sources of data, each with their unique level of uncertainty, are used in the map generation. Sources of error may arise from limitations in acquisition, processing, and interpretation. Moreover, seismic data are collected remotely and the images they provide are derived from generalized mathematical and physical concepts. Consequently, the acquisition that increases the uncertainty includes gaps in coverage because of obstacles to source and receiver deployment, and effect of direction of shooting on data quality (Sheriff and Gelfart, 1995). Processing errors may result from inadequate static corrections, inaccurate velocity analyses, and inappropriate parameter determination.

More specifically to this data set, errors may have also been introduced by the velocity model and its ability to tie formation tops to seismic horizons. The velocity model represents an estimation of the velocity fluctuations for which the accuracy depends on the number of wells and the good fit between time picks and corresponding depths at the well locations. A regression analysis shows that time picks and their corresponding depths at the wells have a strong linearity ( $r^2 = 0.98$ ), meaning that the use of time picks as the external drift in the kriging strategy is justified and accurate. Nevertheless, the uncertainty of the velocity model increases when the distance between the well and any points where velocity is predicted exceed the range of the variogram expressing the spatial dependence between depth and time. In the present case, the range of the different horizons is between 9.5 km and 34 km. The ability to tie formation tops to seismic horizons relies on the successful use of well sonic and density logs, since it is the contrast between the product of these properties for each horizon that generates reflections recorded in seismic exploration. Formation tops used in this study are from Dewing and Embry (2007), for which they mainly utilized gamma-ray logs to position the upper limit of the formation in depth. This error may have been introduced by projecting the formation tops on seismic sections recorded time.

TIME- AND DEPTH-STRUCTURE DATA DISPLAY

The time- and depth-structure data shown on this map were gridded at a cell size of 250 m using Universal kriging. Each map presents a grid with a stretched colour ramp at 20% transparency. Time contours generated from the time-structure grids are shown in black at a 50 m interval, whereas depth contours derived from the depth-structure grid are presented at 100 m intervals.

AWINGAK MAP DESCRIPTIONS

The Late Jurassic Awingak Formation consists of shale, chert, carbonate, and oilstones (Dewing and Embry, 2007, see also Fig. 3). Formation-top data indicate the Awingak Formation consistently overlies the Ringnes Formation and is overlain by either the Deer Bay Formation or the Palaeozoic Member of the Beaufort Formation. In some areas the Awingak Formation can be separated into three members: the Sibre Member, the Hot Weather Member, and the Cape Lockwood Member (Dewing and Embry, 2007). When the Awingak Formation reflection is correlated to formation-top data, the reflection is located below the top of the Awingak formation and above the Ringnes Formation. The reflection was therefore determined to represent a prominent reflection in the top of the Ringnes Formation.

The mapped Awingak Formation reflection extends from the narrowest part of the peninsula near Eldridge and Sheppard bays to near the axis of the Murray Harbour syncline. The data gap west of Eden Bay marks the location of Barrow Dome. Two-way traveltimes of the Awingak Formation increase northward from 160 ms to 1745 ms, or from 185 m to 2719 m. The slope of the horizon ranges from 0 to 2° with steepest slopes (up to 2°) observed between the Drake Point anticline and the Barrow Dome, aligned roughly parallel to the axis of the Murray Harbour syncline. The primary dip azimuth of the horizon is to the north with the exception of the area between the axis of the Drake Point anticline and Maryatt Point syncline, where the surface dips into a depression delimited by the fold axes (Harrison, 1994).

UNCERTAINTY

Quantifying the uncertainty of seismic subsurface maps is difficult since several sources of data, each with their unique level of uncertainty, are used in the map generation. Sources of error may arise from limitations in acquisition, processing, and interpretation. Moreover, seismic data are collected remotely and the images they provide are derived from generalized mathematical and physical concepts. Consequently, the acquisition that increases the uncertainty includes gaps in coverage because of obstacles to source and receiver deployment, and effect of direction of shooting on data quality (Sheriff and Gelfart, 1995). Processing errors may result from inadequate static corrections, inaccurate velocity analyses, and inappropriate parameter determination.

More specifically to this data set, errors may have also been introduced by the velocity model and its ability to tie formation tops to seismic horizons. The velocity model represents an estimation of the velocity fluctuations for which the accuracy depends on the number of wells and the good fit between time picks and corresponding depths at the well locations. A regression analysis shows that time picks and their corresponding depths at the wells have a strong linearity ( $r^2 = 0.98$ ), meaning that the use of time picks as the external drift in the kriging strategy is justified and accurate. Nevertheless, the uncertainty of the velocity model increases when the distance between the well and any points where velocity is predicted exceed the range of the variogram expressing the spatial dependence between depth and time. In the present case, the range of the different horizons is between 9.5 km and 34 km. The ability to tie formation tops to seismic horizons relies on the successful use of well sonic and density logs, since it is the contrast between the product of these properties for each horizon that generates reflections recorded in seismic exploration. Formation tops used in this study are from Dewing and Embry (2007), for which they mainly utilized gamma-ray logs to position the upper limit of the formation in depth. This error may have been introduced by projecting the formation tops on seismic sections recorded time.

TIME- AND DEPTH-STRUCTURE DATA DISPLAY

The time- and depth-structure data shown on this map were gridded at a cell size of 250 m using Universal kriging. Each map presents a grid with a stretched colour ramp at 20% transparency. Time contours generated from the time-structure grids are shown in black at a 50 m interval, whereas depth contours derived from the depth-structure grid are presented at 100 m intervals.

AWINGAK MAP DESCRIPTIONS

The Late Jurassic Awingak Formation consists of shale, chert, carbonate, and oilstones (Dewing and Embry, 2007, see also Fig. 3). Formation-top data indicate the Awingak Formation consistently overlies the Ringnes Formation and is overlain by either the Deer Bay Formation or the Palaeozoic Member of the Beaufort Formation. In some areas the Awingak Formation can be separated into three members: the Sibre Member, the Hot Weather Member, and the Cape Lockwood Member (Dewing and Embry, 2007). When the Awingak Formation reflection is correlated to formation-top data, the reflection is located below the top of the Awingak formation and above the Ringnes Formation. The reflection was therefore determined to represent a prominent reflection in the top of the Ringnes Formation.

The mapped Awingak Formation reflection extends from the narrowest part of the peninsula near Eldridge and Sheppard bays to near the axis of the Murray Harbour syncline. The data gap west of Eden Bay marks the location of Barrow Dome. Two-way traveltimes of the Awingak Formation increase northward from 160 ms to 1745 ms, or from 185 m to 2719 m. The slope of the horizon ranges from 0 to 2° with steepest slopes (up to 2°) observed between the Drake Point anticline and the Barrow Dome, aligned roughly parallel to the axis of the Murray Harbour syncline. The primary dip azimuth of the horizon is to the north with the exception of the area between the axis of the Drake Point anticline and Maryatt Point syncline, where the surface dips into a depression delimited by the fold axes (Harrison, 1994).

UNCERTAINTY

Quantifying the uncertainty of seismic subsurface maps is difficult since several sources of data, each with their unique level of uncertainty, are used in the map generation. Sources of error may arise from limitations in acquisition, processing, and interpretation. Moreover, seismic data are collected remotely and the images they provide are derived from generalized mathematical and physical concepts. Consequently, the acquisition that increases the uncertainty includes gaps in coverage because of obstacles to source and receiver deployment, and effect of direction of shooting on data quality (Sheriff and Gelfart, 1995). Processing errors may result from inadequate static corrections, inaccurate velocity analyses, and inappropriate parameter determination.

More specifically to this data set, errors may have also been introduced by the velocity model and its ability to tie formation tops to seismic horizons. The velocity model represents an estimation of the velocity fluctuations for which the accuracy depends on the number of wells and the good fit between time picks and corresponding depths at the well locations. A regression analysis shows that time picks and their corresponding depths at the wells have a strong linearity ( $r^2 = 0.98$ ), meaning that the use of time picks as the external drift in the kriging strategy is justified and accurate. Nevertheless, the uncertainty of the velocity model increases when the distance between the well and any points where velocity is predicted exceed the range of the variogram expressing the spatial dependence between depth and time. In the present case, the range of the different horizons is between 9.5 km and 34 km. The ability to tie formation tops to seismic horizons relies on the successful use of well sonic and density logs, since it is the contrast between the product of these properties for each horizon that generates reflections recorded in seismic exploration. Formation tops used in this study are from Dewing and Embry (2007), for which they mainly utilized gamma-ray logs to position the upper limit of the formation in depth. This error may have been introduced by projecting the formation tops on seismic sections recorded time.

TIME- AND DEPTH-STRUCTURE DATA DISPLAY

The time- and depth-structure data shown on this map were gridded at a cell size of 250 m using Universal kriging. Each map presents a grid with a stretched colour ramp at 20% transparency. Time contours generated from the time-structure grids are shown in black at a 50 m interval, whereas depth contours derived from the depth-structure grid are presented at 100 m intervals.

AWINGAK MAP DESCRIPTIONS

The Late Jurassic Awingak Formation consists of shale, chert, carbonate, and oilstones (Dewing and Embry, 2007, see also Fig. 3). Formation-top data indicate the Awingak Formation consistently overlies the Ringnes Formation and is overlain by either the Deer Bay Formation or the Palaeozoic Member of the Beaufort Formation. In some areas the Awingak Formation can be separated into three members: the Sibre Member, the Hot Weather Member, and the Cape Lockwood Member (Dewing and Embry, 2007). When the Awingak Formation reflection is correlated to formation-top data, the reflection is located below the top of the Awingak formation and above the Ringnes Formation. The reflection was therefore determined to represent a prominent reflection in the top of the Ringnes Formation.

The mapped Awingak Formation reflection extends from the narrowest part of the peninsula near Eldridge and Sheppard bays to near the axis of the Murray Harbour syncline. The data gap west of Eden Bay marks the location of Barrow Dome. Two-way traveltimes of the Awingak Formation increase northward from 160 ms to 1745 ms, or from 185 m to 2719 m. The slope of the horizon ranges from 0 to 2° with steepest slopes (up to 2°) observed between the Drake Point anticline and the Barrow Dome, aligned roughly parallel to the axis of the Murray Harbour syncline. The primary dip azimuth of the horizon is to the north with the exception of the area between the axis of the Drake Point anticline and Maryatt Point syncline, where the surface dips into a depression delimited by the fold axes (Harrison, 1994).

UNCERTAINTY

Quantifying the uncertainty of seismic subsurface maps is difficult since several sources of data, each with their unique level of uncertainty, are used in the map generation. Sources of error may arise from limitations in acquisition, processing, and interpretation. Moreover, seismic data are collected remotely and the images they provide are derived from generalized mathematical and physical concepts. Consequently, the acquisition that increases the uncertainty includes gaps in coverage because of obstacles to source and receiver deployment, and effect of direction of shooting on data quality (Sheriff and Gelfart, 1995). Processing errors may result from inadequate static corrections, inaccurate velocity analyses, and inappropriate parameter determination.

TIME- AND DEPTH-STRUCTURE DATA DISPLAY

The time- and depth-structure data shown on this map were gridded at a cell size of 250 m using Universal kriging. Each map presents a grid with a stretched colour ramp at 20% transparency. Time contours generated from the time-structure grids are shown in black at a 50 m interval, whereas depth contours derived from the depth-structure grid are presented at 100 m intervals.

AWINGAK MAP DESCRIPTIONS

The Late Jurassic Awingak Formation consists of shale, chert, carbonate, and oilstones (Dewing and Embry, 2007, see also Fig. 3). Formation-top data indicate the Awingak Formation consistently overlies the Ringnes Formation and is overlain by either the Deer Bay Formation or the Palaeozoic Member of the Beaufort Formation. In some areas the Awingak Formation can be separated into three members: the Sibre Member, the Hot Weather Member, and the Cape Lockwood Member (Dewing and Embry, 2007). When the Awingak Formation reflection is correlated to formation-top data, the reflection is located below the top of the Awingak formation and above the Ringnes Formation. The reflection was therefore determined to represent a prominent reflection in the top of the Ringnes Formation.

The mapped Awingak Formation reflection extends from the narrowest part of the peninsula near Eldridge and Sheppard bays to near the axis of the Murray Harbour syncline. The data gap west of Eden Bay marks the location of Barrow Dome. Two-way traveltimes of the Awingak Formation increase northward from 160 ms to 1745 ms, or from 185 m to 2719 m. The slope of the horizon ranges from 0 to 2° with steepest slopes (up to 2°) observed between the Drake Point anticline and the Barrow Dome, aligned roughly parallel to the axis of the Murray Harbour syncline. The primary dip azimuth of the horizon is to the north with the exception of the area between the axis of the Drake Point anticline and Maryatt Point syncline, where the surface dips into a depression delimited by the fold axes (Harrison, 1994).

UNCERTAINTY

Quantifying the uncertainty of seismic subsurface maps is difficult since several sources of data, each with their unique level of uncertainty, are used in the map generation. Sources of error may arise from limitations in acquisition, processing, and interpretation. Moreover, seismic data are collected remotely and the images they provide are derived from generalized mathematical and physical concepts. Consequently, the acquisition that increases the uncertainty includes gaps in coverage because of obstacles to source and receiver deployment, and effect of direction of shooting on data quality (Sheriff and Gelfart, 1995). Processing errors may result from inadequate static corrections, inaccurate velocity analyses, and inappropriate parameter determination.

TIME- AND DEPTH-STRUCTURE DATA DISPLAY

The time- and depth-structure data shown on this map were gridded at a cell size of 250 m using Universal kriging. Each map presents a grid with a stretched colour ramp at 20% transparency. Time contours generated from the time-structure grids are shown in black at a 50 m interval, whereas depth contours derived from the depth-structure grid are presented at 100 m intervals.

AWINGAK MAP DESCRIPTIONS

The Late Jurassic Awingak Formation consists of shale, chert, carbonate, and oilstones (Dewing and Embry, 2007, see also Fig. 3). Formation-top data indicate the Awingak Formation consistently overlies the Ringnes Formation and is overlain by either the Deer Bay Formation or the Palaeozoic Member of the Beaufort Formation. In some areas the Awingak Formation can be separated into three members: the Sibre Member, the Hot Weather Member, and the Cape Lockwood Member (Dewing and Embry, 2007). When the Awingak Formation reflection is correlated to formation-top data, the reflection is located below the top of the Awingak formation and above the Ringnes Formation. The reflection was therefore determined to represent a prominent reflection in the top of the Ringnes Formation.

The mapped Awingak Formation reflection extends from the narrowest part of the peninsula near Eldridge and Sheppard bays to near the axis of the Murray Harbour syncline. The data gap west of Eden Bay marks the location of Barrow Dome. Two-way traveltimes of the Awingak Formation increase northward from 160 ms to 1745 ms, or from 185 m to 2719 m. The slope of the horizon ranges from 0 to 2° with steepest slopes (up to 2°) observed between the Drake Point anticline and the Barrow Dome, aligned roughly parallel to the axis of the Murray Harbour syncline. The primary dip azimuth of the horizon is to the north with the exception of the area between the axis of the Drake Point anticline and Maryatt Point syncline, where the surface dips into a depression delimited by the fold axes (Harrison, 1994).

UNCERTAINTY

Quantifying the uncertainty of seismic subsurface maps is difficult since several sources of data, each with their unique level of uncertainty, are used in the map generation. Sources of error may arise from limitations in acquisition, processing, and interpretation. Moreover, seismic data are collected remotely and the images they provide are derived from generalized mathematical and physical concepts. Consequently, the acquisition that increases the uncertainty includes gaps in coverage because of obstacles to source and receiver deployment, and effect of direction of shooting on data quality (Sheriff and Gelfart, 1995). Processing errors may result from inadequate static corrections, inaccurate velocity analyses, and inappropriate parameter determination.

TIME- AND DEPTH-STRUCTURE DATA DISPLAY

The time- and depth-structure data shown on this map were gridded at a cell size of 250 m using Universal kriging. Each map presents a grid with a stretched colour ramp at 20% transparency. Time contours generated from the time-structure grids are shown in black at a 50 m interval, whereas depth contours derived from the depth-structure grid are presented at 100 m intervals.

AWINGAK MAP DESCRIPTIONS

The Late Jurassic Awingak Formation consists of shale, chert, carbonate, and oilstones (Dewing and Embry, 2007, see also Fig. 3). Formation-top data indicate the Awingak Formation consistently overlies the Ringnes Formation and is overlain by either the Deer Bay Formation or the Palaeozoic Member of the Beaufort Formation. In some areas the Awingak Formation can be separated into three members: the Sibre Member, the Hot Weather Member, and the Cape Lockwood Member (Dewing and Embry, 2007). When the Awingak Formation reflection is correlated to formation-top data, the reflection is located below the top of the Awingak formation and above the Ringnes Formation. The reflection was therefore determined to represent a prominent reflection in the top of the Ringnes Formation.

The mapped Awingak Formation reflection extends from the narrowest part of the peninsula near Eldridge and Sheppard bays to near the axis of the Murray Harbour syncline. The data gap west of Eden Bay marks the location of Barrow Dome. Two-way traveltimes of the Awingak Formation increase northward from 160 ms to 1745 ms, or from 185 m to 2719 m. The slope of the horizon ranges from 0 to 2° with steepest slopes (up to 2°) observed between the Drake Point anticline and the Barrow Dome, aligned roughly parallel to the axis of the Murray Harbour syncline. The primary dip azimuth of the horizon is to the north with the exception of the area between the axis of the Drake Point anticline and Maryatt Point syncline, where the surface dips into a depression delimited by the fold axes (Harrison, 1994).

UNCERTAINTY

Quantifying the uncertainty of seismic subsurface maps is difficult since several sources of data, each with their unique level of uncertainty, are used in the map generation. Sources of error may arise from limitations in acquisition, processing, and interpretation. Moreover, seismic data are collected remotely and the images they provide are derived from generalized mathematical and physical concepts. Consequently, the acquisition that increases the uncertainty includes gaps in coverage because of obstacles to source and receiver deployment, and effect of direction of shooting on data quality (Sheriff and Gelfart, 1995). Processing errors may result from inadequate static corrections, inaccurate velocity analyses, and inappropriate parameter determination.

TIME- AND DEPTH-STRUCTURE DATA DISPLAY

The time- and depth-structure data shown on this map were gridded at a cell size of 250 m using Universal kriging. Each map presents a grid with a stretched colour ramp at 20% transparency. Time contours generated from the time-structure grids are shown in black at a 50 m interval, whereas depth contours derived from the depth-structure grid are presented at 100 m intervals.

AWINGAK MAP DESCRIPTIONS

The Late Jurassic Awingak Formation consists of shale, chert, carbonate, and oilstones (Dewing and Embry, 2007, see also Fig. 3). Formation-top data indicate the Awingak Formation consistently overlies the Ringnes Formation and is overlain by either the Deer Bay Formation or the Palaeozoic Member of the Beaufort Formation. In some areas the Awingak Formation can be separated into three members: the Sibre Member, the Hot Weather Member, and the Cape Lockwood Member (Dewing and Embry, 2007). When the Awingak Formation reflection is correlated to formation-top data, the reflection is located below the top of the Awingak formation and above the Ringnes Formation. The reflection was therefore determined to represent a prominent reflection in the top of the Ringnes Formation.

The mapped Awingak Formation reflection extends from the narrowest part of the peninsula near Eldridge and Sheppard bays to near the axis of the Murray Harbour syncline. The data gap west of Eden Bay marks the location of Barrow Dome. Two-way traveltimes of the Awingak Formation increase northward from 160 ms to 1745 ms, or from 185 m to 2719 m. The slope of the horizon ranges from 0 to 2° with steepest slopes (up to 2°) observed between the Drake Point anticline and the Barrow Dome, aligned roughly parallel to the axis of the Murray Harbour syncline. The primary dip azimuth of the horizon is to the north with the exception of the area between the axis of the Drake Point anticline and Maryatt Point syncline, where the surface dips into a depression delimited by the fold axes (Harrison, 1994).

UNCERTAINTY

Quantifying the uncertainty of seismic subsurface maps is difficult since several sources of data, each with their unique level of uncertainty, are used in the map generation. Sources of error may arise from limitations in acquisition, processing, and interpretation. Moreover, seismic data are collected remotely and the images they provide are derived from generalized mathematical and physical concepts. Consequently, the acquisition that increases the uncertainty includes gaps in coverage because of obstacles to source and receiver deployment, and effect of direction of shooting on data quality (Sheriff and Gelfart, 1995). Processing errors may result from inadequate static corrections, inaccurate velocity analyses, and inappropriate parameter determination.

TIME- AND DEPTH-STRUCTURE DATA DISPLAY

The time- and depth-structure data shown on this map were gridded at a cell size of 250 m using Universal kriging. Each map presents a grid with a stretched colour ramp at 20% transparency. Time contours generated from the time-structure grids are shown in black at a 50 m interval, whereas depth contours derived from the depth-structure grid are presented at 100 m intervals.

AWINGAK MAP DESCRIPTIONS

The Late Jurassic Awingak Formation consists of shale, chert, carbonate, and oilstones (Dewing and Embry, 2007, see also Fig. 3). Formation-top data indicate the Awingak Formation consistently overlies the Ringnes Formation and is overlain by either the Deer Bay Formation or the Palaeozoic Member of the Beaufort Formation. In some areas the Awingak Formation can be separated into three members: the Sibre Member, the Hot Weather Member, and the Cape Lockwood Member (Dewing and Embry, 2007). When the Awingak Formation reflection is correlated to formation-top data, the reflection is located below the top of the Awingak formation and above the Ringnes Formation. The reflection was therefore determined to represent a prominent reflection in the top of the Ringnes Formation.

The mapped Awingak Formation reflection extends from the narrowest part of the peninsula near Eldridge and Sheppard bays to near the axis of the Murray Harbour syncline. The data gap west of Eden Bay marks the location of Barrow Dome. Two-way traveltimes of the Awingak Formation increase northward from 160 ms to 1745 ms, or from 185 m to 2719 m. The slope of the horizon ranges from 0 to 2° with steepest slopes (up to 2°) observed between the Drake Point anticline and the Barrow Dome, aligned roughly parallel to the axis of the Murray Harbour syncline. The primary dip azimuth of the horizon is to the north with the exception of the area between the axis of the Drake Point anticline and Maryatt Point syncline, where the surface dips into a depression delimited by the fold axes (Harrison, 1994).

UNCERTAINTY

Quantifying the uncertainty of seismic subsurface maps is difficult since several sources of data, each with their unique level of uncertainty, are used in the map generation. Sources of error may arise from limitations in acquisition, processing, and interpretation. Moreover, seismic data are collected remotely and the images they provide are derived from generalized mathematical and physical concepts. Consequently, the acquisition that increases the uncertainty includes gaps in coverage because of obstacles to source and receiver deployment, and effect of direction of shooting on data quality (Sheriff and Gelfart, 1995). Processing errors may result from inadequate static corrections, inaccurate velocity analyses, and inappropriate parameter determination.

TIME- AND DEPTH-STRUCTURE DATA DISPLAY

The time- and depth-structure data shown on this map were gridded at a cell size of 250 m using Universal kriging. Each map presents a grid with a stretched colour ramp at 20% transparency. Time contours generated from the time-structure grids are shown in black at a 50 m interval, whereas depth contours derived from the depth-structure grid are presented at 100 m intervals.

AWINGAK MAP DESCRIPTIONS

The Late Jurassic Awingak Formation consists of shale, chert, carbonate, and oilstones (Dewing and Embry, 2007, see also Fig. 3). Formation-top data indicate the Awingak Formation consistently overlies the Ringnes Formation and is overlain by either the Deer Bay Formation or the Palaeozoic Member of the Beaufort Formation. In some areas the Awingak Formation can be separated into three members: the Sibre Member, the Hot Weather Member, and the Cape Lockwood Member (Dewing and Embry, 2007). When the Awingak Formation reflection is correlated to formation-top data, the reflection is located below the top of the Awingak formation and above the Ringnes Formation. The reflection was therefore determined to represent a prominent reflection in the top of the Ringnes Formation.

The mapped Awingak Formation reflection extends from the narrowest part of the peninsula near Eldridge and Sheppard bays to near the axis of the Murray Harbour syncline. The data gap west of Eden Bay marks the location of Barrow Dome. Two-way traveltimes of the Awingak Formation increase northward from 160 ms to 1745 ms, or from 185 m to 2719 m. The slope of the horizon ranges from 0 to 2° with steepest slopes (up to 2°) observed between the Drake Point anticline and the Barrow Dome, aligned roughly parallel to the axis of the Murray Harbour syncline. The primary dip azimuth of the horizon is to the north with the exception of the area between the axis of the Drake Point anticline and Maryatt Point syncline, where the surface dips into a depression delimited by the fold axes (Harrison, 1994).

UNCERTAINTY

Quantifying the uncertainty of seismic subsurface maps is difficult since several sources of data, each with their unique level